

A HIGH SELECTIVITY DUAL-BAND BANDPASS FILTER USING DUAL-MODE AND TRIPLE-MODE RESONATORS

Xiaoguo Huang, Quanyuan Feng^{*}, QianYin Xiang, and Dinghong Jia

School of Information Science and Technology, Southwest Jiaotong University, Chengdu, Sichuan 610031, China

Abstract—In this paper, a novel high selectivity dual-band microwave bandpass filter (BPF) using dual-mode and triple-mode resonator is proposed. First, a dual-band filter comprising two dual-mode single band filters using common input/out lines is designed. Each single BPF is realized using a stepped-impedance resonator (SIR) with a centrally-loaded shunt open stub. The first and second passband can be independently controlled by the two dual-mode resonators, respectively. The proposed filter also offers three transmission zeros (TZs) to improve the selectivity. To further improve the selectivity over high side band of the first passband, a novel triple-mode resonator is designed to replace the dual-mode resonator. The basic structure of triple-mode resonator is microstrip-to-coplanar waveguide (CPW) structure. The microstrip structure provides one odd mode and one even mode resonant frequency and the CPW structure can provide another even mode resonant frequency without increasing circuit size. Both simulated and measured results show that the filters exhibit a good performance, including a small insertion loss, selectivity.

1. INTRODUCTION

Due to the rapid development of wireless communication technology, microwave filters with dual-band, high frequency selectivity and compact size are highly demanded to the multi-mode communication system [1–3]. For example, global system for mobile communications (GSM) and wireless local area networks (WLANs) standards. Thus, much research regarding dual-band filters has been carried out.

Received 17 December 2012, Accepted 5 January 2013, Scheduled 9 January 2013

* Corresponding author: Quanyuan Feng (fengquanyuan@163.com).

Among them, there are mainly three typical methods. The first one is to combine two sets of different resonators with common input and output [4–7]. Those resonators can be realized using multi-mode resonator [4, 5] or single mode resonator [6, 7]. In [4], two triple-mode resonators were designed on multi-layered to achieve high selectivity. In [6, 7], the single mode resonator achieves high selectivity by cross-coupling technology. These filters have the advantages of two independent passbands, high selectivity and simple design procedure. However, the requirement on larger circuit size arises due to the two filtering circuits.

The second method is to utilize a single resonator by properly controlling second mode or first harmonic [8–14]. In [8–13], dual-band filters are realized by a single dual-mode resonator with controllable first harmonic. In [14], a E-shaped SIR resonator is used to design single mode dual-band filter. These filters are with small circuit size, but they usually have a poor selectivity comparing first method and the second passbands are always affected by the first passbands.

The last method to achieve a dual-band performance is employing the resonators consisting of the open- or short-circuit stubs [15–17], which are placed in series or in parallel to create TZs in the middle passband of a wideband BPF. These circuits present high skirt selectivity, but they usually require a complex design procedure and have a larger circuit area due to the many series or shunt stubs.

In this paper, we propose a dual-band BPF based on two microstrip dual-mode resonators with common input and output, which shows three TZs in the desired band. Then, to improve the selectivity of the first band, another TZ is created on the high side of the first passband by adding CPW structure into microstrip dual-mode resonator. The microstrip-to-CPW structure can be considered as a triple-mode resonator because of three resonant frequencies in the first passband. Details of dual-band filter design are presented and measured results are given to demonstrate the performance of the proposed filter.

2. DUAL-BAND BANDPASS FILTER I BASED ON TWO DUAL-MODE RESONATORS

Figure 1 shows the proposed dual-mode dual-band BPF. It consists of two single-band BPFs combined with common input and output ports. Each single-band BPF comprised dual-mode resonators that contain a SIR with a centrally-loaded shunt open stub. The coupling scheme of the proposed filter is shown in Figure 2, where S and L denote input and output ports, respectively. Nodes 1 and 2 denote the two modes

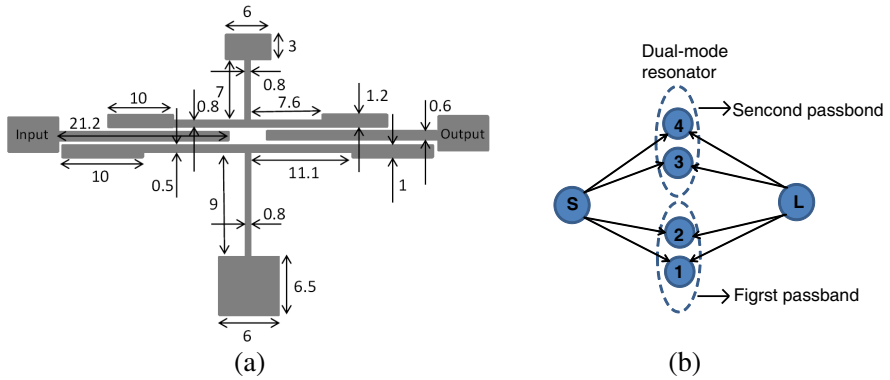


Figure 1. (a) The schematic of the proposed dual-band filter I based on two dual-mode resonators. (b) Coupling scheme of the proposed filter.

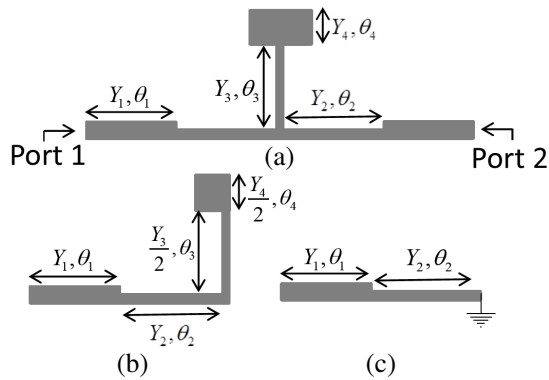


Figure 2. (a) Basic structure of the proposed dual-mode resonator. (b) Even-mode excitation equivalent circuit. (c) Odd-mode excitation equivalent circuit. In this design, the parameters of the top dual-mode resonator are: $Y_{1t} = 0.018 \text{ S}$, $\theta_{1t} = 35^\circ$, $Y_{2t} = 0.014 \text{ S}$, $\theta_{2t} = 27^\circ$, $Y_{3t} = 0.014 \text{ S}$, $\theta_{3t} = 24^\circ$, $Y_{4t} = 0.062 \text{ S}$ and $\theta_{4t} = 11^\circ$. The parameters of the bottom dual-mode resonator are: $Y_{1b} = 0.017 \text{ S}$, $\theta_{1b} = 35^\circ$, $Y_{2b} = 0.011 \text{ S}$, $\theta_{2b} = 38^\circ$, $Y_{3b} = 0.014 \text{ S}$, $\theta_{3b} = 31^\circ$, $Y_{4b} = 0.062 \text{ S}$ and $\theta_{4b} = 24^\circ$.

created by the bottom dual-mode resonator and nodes 3 and 4 denote the two modes created by the top dual-mode resonator at the first and second band center frequencies, respectively.

The basic structure of the proposed dual-mode resonator is shown

in Figure 2(a). It can be divided using the symmetrical plane, one of which is regarded as an open circuit or a short circuit for even or odd modes, respectively. In the even mode, $Y_3/2$ and $Y_4/2$ result from dividing the stepped-impedance stubs in half along the plane of symmetry, as shown in Figure 2(b). In the odd mode, because the plane of symmetry can be considered as ground plane, a simple equivalent circuit is made as shown in Figure 2(c). The resonance frequencies can be calculated when $\text{Im}[Y_{\text{in_even}}] = 0$ and $\text{Im}[Y_{\text{in_odd}}] = 0$ from the one end of the even- and odd-mode circuit, respectively, which can be expressed by

$$Y_2 \frac{Y_3 (Y_4 \tan \theta_4 + Y_3 \tan \theta_3) + 2Y_2 (Y_3 - Y_4 \tan \theta_4 \tan \theta_3) \tan \theta_2}{2Y_2 (Y_3 - Y_4 \tan \theta_4 \tan \theta_3) - Y_3 (Y_4 \tan \theta_4 + Y_3 \tan \theta_3) \tan \theta_2} + Y_1 \tan \theta_1 = 0 \quad \text{for even mode} \quad (1)$$

and

$$-jY_2 \cot \theta_2 + jY_1 \tan \theta_1 = 0 \quad \text{for odd mode} \quad (2)$$

The TZ frequencies are obtained when $Y_{21} = Y_{12} = 0$, where the admittance matrices are calculated by Y -parameter between port 1 and port 2 in Figure 2(a). Assuming $Y_1 = Y_2 = Y_0$ and $\theta_1 + \theta_2 = \theta_0$, the filter TZs can be calculated by

$$Y_{12} = Y_{21} = \frac{-1}{j \frac{1}{Y_1} \cos \theta_0 \sin \theta_0 + \frac{1}{Y_1} j \sin \theta_0 \left(\cos \theta_0 + j \frac{Y_{\text{load}}}{Y_1} \right)} = 0 \quad (3)$$

where $Y_{\text{load}} = \frac{jY_3 \sin \theta_3 \cos \theta_4 + jY_4 \cos \theta_3 \sin \theta_4}{\cos \theta_3 \cos \theta_4 - \frac{Y_4}{Y_3} \sin \theta_3 \sin \theta_4}$ thus, $Y_{\text{load}} \rightarrow \infty$ can be deduced and

$$Y_3 - Y_4 \tan \theta_4 \tan \theta_3 = 0 \quad (4)$$

From (1), (2) and (4), it can be observed that the odd-mode resonant frequency depends on Y_1 , Y_2 , θ_1 and θ_2 , and the even-mode resonant frequency depends on Y_1 , Y_2 , Y_3 , Y_4 , θ_1 , θ_2 , θ_3 and θ_4 . It also can be seen that the TZ just depends on Y_3 , Y_4 , θ_3 and θ_4 . To verify the theoretical analysis, a full-wave electromagnetics simulation was carried out using Sonnet. Figure 3 shows the simulated S_{21} -magnitude of a weak coupling resonator circuit according to different Y_{1b} , θ_{4b} , Y_{1t} and θ_{4t} , where the subscript b and t represent the bottom dual-mode resonator and the top dual-mode resonator. As Y_{1b} or Y_{1t} is varied, the odd- and even-mode resonant frequencies are tuned simultaneously, whereas θ_{4b} or θ_{4t} is varied, the odd-mode resonant frequency is fixed and the even-mode resonant frequency can be tuned. Thus, the even and odd modes do not couple to each other. Moreover, the two passbands are independent. This characteristic can be utilized in the design of dual-band BPF with independently two passbands.

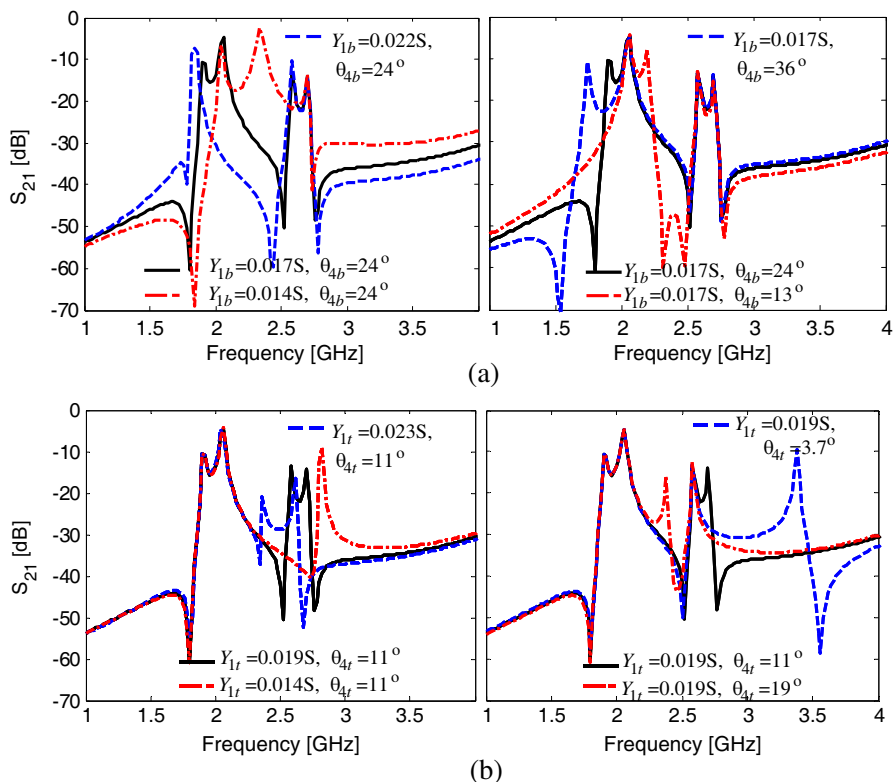


Figure 3. (a) Resonant frequency according to Y_{1b} and θ_{4b} and (b) resonant frequency according to Y_{1t} and θ_{4t} .

Figure 4 shows simulated S_{21} -magnitude of a weak coupling resonator circuit under different orders of odd-even-modes, where odd_b and even_b denote the odd and even mode provided by the bottom dual-mode resonator and odd_t and even_t denote the odd and even mode provided by the top dual-mode resonator as shown in Figure 1(a). The orders of odd-even-modes are controlled by electrical length of θ_{4b} and θ_{4t} . It can be observed that Figure 4(a) has the best selectivity because of one TZ located at lower first passband, one TZ located between two passbands and one TZ located at higher second passband. Figure 4(b) shows a better selectivity between first and second passband. However, poor selectivity exists at the low frequency. There are only two TZs in the desired band, which resulting in poor selectivity, as shown in Figure 4(c) and Figure 4(d). Thus, the order of modes in Figure 4(a) is chosen to design dual-mode filter in this

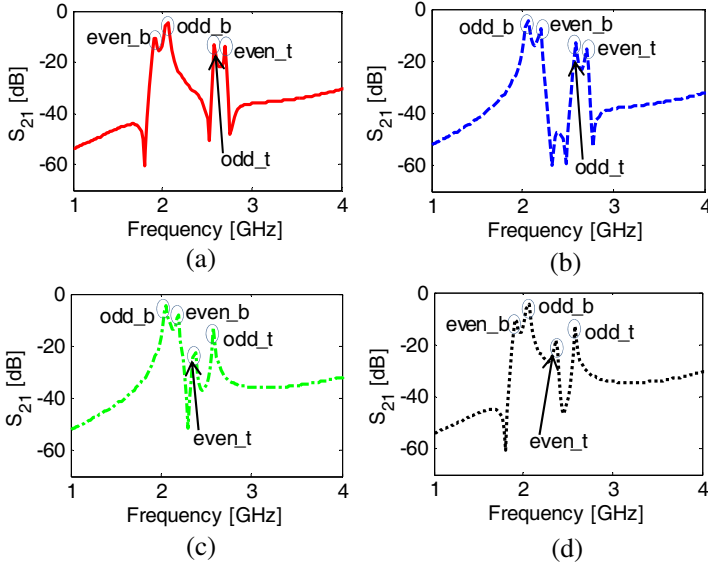


Figure 4. S_{21} -magnitude under different orders of odd-even-modes. (a) $\theta_{4b} = 24^\circ$, $\theta_{4t} = 11^\circ$; (b) $\theta_{4b} = 13^\circ$, $\theta_{4t} = 11^\circ$; (c) $\theta_{4b} = 13^\circ$, $\theta_{4t} = 4^\circ$; (d) $\theta_{4b} = 24^\circ$, $\theta_{4t} = 4^\circ$.

design.

To verify the analytical of the proposed dual-mode resonators, a dual-band BPF is designed, simulated, and measured on the F4B-2 substrate with a dielectric constant of 2.65 and thickness of 0.5 mm. The simulated and measured results are illustrated in Figure 5. The measured results agree well with simulated results. Measured results show that the first passband and second passband, which are centered at 2.0 and 2.65 GHz, exhibit an insertion loss of < 0.6 dB and < 0.9 dB, and a return loss of > 19 dB and > 19 dB, respectively. There are three TZs in the desired band, which are located at 1.84 GHz, 2.46 GHz, and 2.81 GHz, respectively.

3. DUAL-BAND BANDPASS FILTER II BASED ON DUAL-MODE AND TRIPLE-MODE RESONATOR

To improve the selectivity of the first band, a new triplemode resonator is proposed using microstrip-to-CPW structure as shown in Figure 6. The CPW structure connected to microstrip structure by a via can provide another TZ between the passbands to enhance the isolation. The microstrip structure of the filter II has the same design

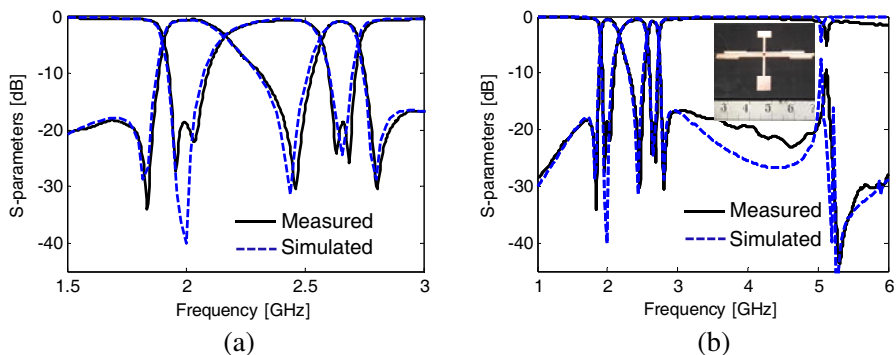


Figure 5. Simulated, measured results and the photograph of the dual-band BPF I. (a) Narrowband and (b) wideband.

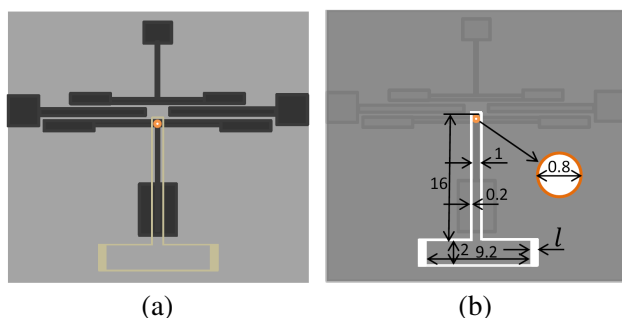


Figure 6. The schematic of the proposed dual-band filter II based on dual-mode resonator and triplemode resonator. (a) Top view. (b) Bottom view.

specifications as filter I, and its configuration is presented in Figure 6. Figure 7 shows the simulated S_{21} parameters under different values of l . It can be seen that the CPW structure can provide another resonant frequency to first passband, and it can be easily tuned by l . In this design, 0.8 mm is chosen to the length of l . Four TZs are observed in the desired band, one locates at the low side of first band, two TZs are brought in between the first and second band, the other is at the high side of second band, which leads to a high selectivity.

The dual-band filter II has also been fabricated on a 0.5 mm F4B-2 substrate with a relative dielectric constant of 2.65 and its photograph is presented in Figure 8. The filtering performance is measured by an Agilent network analyzer E5071C. The measured frequency responses of insertion and return losses are shown in Figure 9. Clearly, measured results agree well with the simulated ones. Measured results show

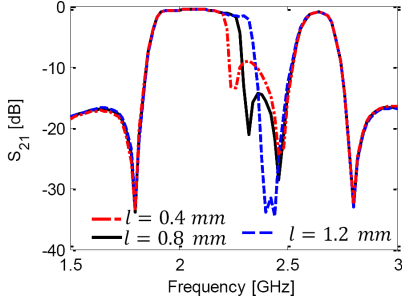


Figure 7. S_{21} parameter under different values of l .

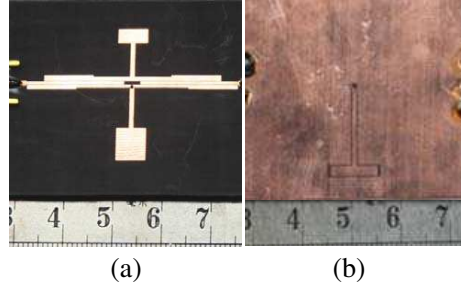


Figure 8. Photograph of the fabricated dual-band BPF II. (a) Top view. (b) Bottom view.

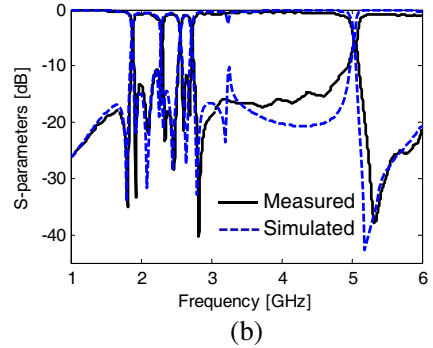
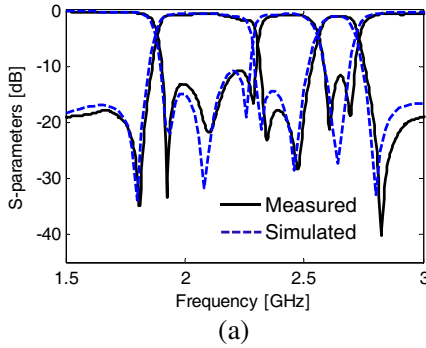


Figure 9. Simulated, measured results and the photograph of the dual-band BPF II. (a) Narrowband and (b) wideband.

that the first and second passband, which are centered at 2.0 and 2.65 GHz with a fraction bandwidth of 20.5% and 6%, respectively, have a minimum insertion loss of < 0.6 and < 1.1 dB, and have return loss of > 11 dB and > 13 dB, respectively. In addition, the filter has four TZs at 1.8 GHz with 34 dB rejection, 2.35 GHz with 23 dB rejection, 2.48 GHz with 29 dB rejection, 2.82 GHz with 40 dB rejection, respectively. These TZs improve the rejection level in the stopband and greatly improves passbands selectivity.

4. CONCLUSIONS

In this paper, firstly, a novel microstrip dual-band filter with three TZs using two SIR dual-mode resonators is demonstrated. To improve the selectivity of the first passband, a novel triplemode resonator

using microstrip-to-CPW structure is proposed to replace the dual mode resonator. The proposed dual-mode filters are validated by both theoretical analysis and experiments. The prototype with an overall size of $44.2 \text{ mm} \times 30 \text{ mm} \times 0.5 \text{ mm}$ has been analyzed, designed, fabricated and measured. The measured results are in good agreement with the theoretical predictions. The proposed microstrip-to-CPW structure can be applicable to design high performance filter with compact size.

ACKNOWLEDGMENT

This work was partly supported by the National Natural Science Foundation of China (NNSF) under Grant 60990320, 60990323, 61271090, the National 863 Project of China under Grant 2012AA012305, Sichuan Provincial Science and technology support Project under Grant 2012GZ0101, Chengdu Science and technology support Project under Grant 12DXYB347JH-002, and the “2013 Doctoral Innovation Funds of Southwest Jiaotong University” and “the Fundamental Research Funds for the Central Universities”.

REFERENCES

1. Chen, C. Y. and C. C. Lin, “The design and fabrication of a highly compact microstrip dual-band bandpass filter,” *Progress In Electromagnetics Research*, Vol. 112, 299–307, 2011.
2. Velazquez-Ahumada, M. D. C., “Application of stub loaded folded stepped impedance resonators to dual band filter design,” *Progress In Electromagnetics Research*, Vol. 102, 107–124, 2010.
3. Kuo, J. T. and S. W. Lai, “New dual-band bandpass filter with wide upper rejection band,” *Progress In Electromagnetics Research*, Vol. 123, 371–384, 2012.
4. Wu, H. W., Y. F. Chen, and Y. F. Chen, “Multi-layered dual-band bandpass filter using stub-loaded stepped-impedance and uniform-impedance resonators,” *IEEE Microw. Wireless Compon. Lett.*, Vol. 22, No. 3, 114–116, Mar. 2012.
5. Wang, J., L. Ge, K. Wang, and W. Wu, “Compact microstrip dual-mode dual-band bandpass filter with wide stopband,” *Electronics Letters*, Vol. 47, No. 4, Feb. 2011.
6. Chen, C. F., T. Y. Huang, and R. B. Wu, “Design of dual- and triple-passband filters using alternately cascaded multiband resonators,” *IEEE Trans. on Microw. Theory and Tech.*, Vol. 54, No. 9, 3550–3558, Sep. 2006.

7. Deng, P. H. and J. H. Jheng, "A switched reconfigurable high-isolation dual-band bandpass filter," *IEEE Microw. Wireless Compon. Lett.*, Vol. 21, No. 2, 71–73, Feb. 2012.
8. Xu, J., C. Miao, and W. Wu, "A compact and high isolation dual-mode dual-band bandpass filter with tunable transmission zeros," *Journal of Electromagnetic Waves and Applications*, Vol. 26, Nos. 17–18, 2390–2397, Dec. 2012.
9. Wei, F., L. Chen, and X. W. Shi, "Compact dual-mode dual-band bandpass filter with wide stopband," *Journal of Electromagnetic Waves and Applications*, Vol. 26, Nos. 11–12, 1441–1447, Aug. 2012.
10. Deng, H. W., Y. J. Zhao, X. S. Zhang, W. Chen, and J. K. Wang, "Compact and high selectivity dual-band dual-mode microstrip BPF with single step-impedance resonator," *Electronics Letters*, Vol. 47, No. 5, Mar. 2011.
11. Youngje, S., "Dual-mode dual-band filter with band notch structures," *IEEE Microw. Wireless Compon. Lett.*, Vol. 20, No. 2, 73–75, Jan. 2010.
12. Sun, S., "A dual-band bandpass filter using a single dual-mode ring resonator," *IEEE Microw. Wireless Compon. Lett.*, Vol. 21, No. 6, 298–300, Jun. 2011.
13. Lee, J. and Y. Lim, "Compact dual-band bandpass filter with good frequency selectivity," *Electronics Letters*, Vol. 47, No. 25, Dec. 2011.
14. Wu, Y. L., C. Liao, and X. Z. Xiong, "A dual-wideband bandpass filter based on E-shaped microstrip SIR with improved upper stopband performance," *Progress In Electromagnetics Research*, Vol. 108, 141–153, 2010.
15. Chang, W. S. and C. Y. Chang, "Analytical design of microstrip short-circuit terminated stepped-impedance resonator dual-band filters," *IEEE Trans. on Microw. Theory and Tech.*, Vol. 59, No. 7, 1730–1739, Jul. 2011.
16. Mashhadi, M. and N. Komjani, "Design of novel dual-band bandpass filter with multi-spurious suppression for WLAN application," *Journal of Electromagnetic Waves and Applications*, Vol. 26, No. 7, 851–862, 2012.
17. Seungku, L. and L. Yongshik, "A planar dual-band filter based on reduced-length parallel coupled lines," *IEEE Microw. Wireless Compon. Lett.*, Vol. 20, No. 1, 16–18, Jan. 2010.